Systematic study of the superconducting and normal-state properties of neutron-irradiated MgB_2

R. H. T. Wilke, S. L. Bud'ko, and P. C. Canfield
Ames Laboratory US DOE and Department of Physics and Astronomy, Iowa State University, Ames, Iowa 50011, USA

J. Farmer
Missouri University Research Reactor, University of Missouri–Columbia, Research Park, Columbia, Missouri 65211, USA

S. T. Hannahs
National High Magnetic Field Laboratory, Florida State University, 1800 E. Paul Dirac Drive, Tallahassee, Florida 32310, USA
(Received 7 July 2005; revised manuscript received 16 February 2006; published 14 April 2006)

We have performed a systematic study of the evolution of the superconducting and normal state properties of neutron-irradiated MgB_2 wire segments as a function of fluence and post exposure annealing temperature and time. All fluences used suppressed the transition temperature, T_c, below 5 K and expanded the unit cell. For each annealing temperature T_c recovers with annealing time and the upper critical field, $H_{c2}(T=0)$, approximately scales with T_c. By judicious choice of fluence, annealing temperature, and time, the T_c of damaged MgB_2 can be tuned to virtually any value between 5 and 39 K. For higher annealing temperatures and longer annealing times, the recovery of T_c tends to coincide with a decrease in the normal state resistivity and a systematic recovery of the lattice parameters.

DOI: 10.1103/PhysRevB.73.134512 PACS number(s): 74.70−b, 74.25.Fy, 74.25.Ha, 74.25.Sv

I. INTRODUCTION

It has been well established that superconductivity near 40 K[1] in MgB_2 is phonon mediated[2,3] with two distinct energy gaps[4] (see Ref. 5 and works therein for a review of the basic properties of MgB_2). Much recent work has focused on understanding how structural defects and chemical substitutions affect the superconducting properties. The goal is twofold; first, to understand the basic physics in this unique system and, second, to use this understanding as a basis for developing practical superconducting wires, tapes, or devices.

Of the many elements investigated, only Al and C have shown concrete evidence of entering the structure.[6] Both electron-dope the system and it is the Fermi surface changes, rather than interband scattering, which are believed to cause the suppression of T_c.[3,7] When aluminum substitutes for magnesium, $H_{c2}^{\|ab}$ decreases while $H_{c2}^{\perp ab}$ remains constant or slightly increases, resulting in a decrease in the anisotropy ratio, $\gamma_H = H_{c2}^{\|ab}/H_{c2}^{\perp ab}$.[7–9] These changes can be understood as the result of changes in the Fermi surface topology of the σ band.[10] In the case of carbon substitution for boron, the upper critical field is enhanced in both directions,[11,12] with $H_{c2}^{\perp ab}$ increasing more rapidly than $H_{c2}^{\|ab}$, leading to a decrease in the anisotropy ratio.[7] This enhancement of the upper critical field cannot be explained in terms of changes in the Fermi surface and is believed to result from an increase the scattering in the π band,[7] in accordance with the theory proposed by Gurevich.[13]

Damaging or disordering of the sample using protons, heavy ions, neutrons, etc., is another route to systematically changing the system. Of these possible routes, neutron irradiation offers the best avenue for uniformly damaging bulk MgB_2. There are two main sources of damage from neutron irradiation of MgB_2. First, fast neutrons deposit energy through inelastic collisions with atoms, creating thermal and dislocation spikes.[14] Second, ^{10}B has a large capture cross section for lower energy neutrons and readily absorbs these thermal neutrons, subsequently α-decaying to ^7Li. Early neutron damage studies focused on the irradiation of powders or pressed pellets of MgB_2 containing natural boron.[15–18]

The absorption of slow neutrons by ^{10}B can lead to self shielding and prevents uniform damage in bulk MgB_2 samples significantly larger than the penetration depth. Under the assumption of linear absorption, the intensity of the incident beam decreases exponentially within the sample, and is given by[19]

$$I(t) = I_0 \exp(-tsN), \tag{1}$$

where I_0 is the initial intensity, t is the sample depth, s is the absorption cross section, and N is the number density of atoms. Here, N corresponds to the number of ^{10}B atoms per cm^3. A calculation of the half depth in MgB_2 synthesized from natural boron, which consists of 19.9% ^{10}B, yields a depth of approximately 130 μm. Samples with dimensions significantly larger than 130 μm will contain substantial gradients of damage associated with slow neutron absorption. Therefore several different approaches have been employed to minimize neutron capture, ensuring homogeneous damage throughout bulk samples. Thermal neutrons have been blocked by a cadmium shield[16,20,21] or the natural boron has been replaced with isotopically enriched ^{11}B.[22,23]

An alternate approach is to damage MgB_2 objects with characteristic dimensions comparable to or smaller than 130 μm. In this case natural boron can be used and relatively homogeneous absorption of slow neutrons can be assumed. In this paper we report on the isotropic irradiation of fully dense, 140 μm diameter, MgB_2 wires with both thermal and fast neutrons. Although these fibers contain natural boron, they were exposed to an isotropic fluence and had sample dimensions comparable to the penetration length, implying

TABLE I. Estimated fluences for each of the four exposure times and calculated atomic percentage of boron transmutated to lithium.

Exposure time (hours)	Fluence (cm^{-2})	Atomic % Li
24	4.75×10^{18}	0.37
48	9.50×10^{18}	0.74
72	1.43×10^{19}	1.11
96	1.90×10^{19}	1.48

the defect structure should be fairly uniform throughout the samples.

II. EXPERIMENTAL METHODS

We synthesized fully dense, 140 μm diameter MgB_2 wire by reacting boron filaments with magnesium vapor at 950 °C for 36 h. This technique is described in full detail elsewhere.[24] Once synthesized, three fibers, each approximately 1–2 cm in length, were sealed under a partial helium atmosphere in quartz ampoules with dimensions of 3 mm I.D., 4 mm O.D., and approximately 3 cm long. A partial atmosphere of inert gas was necessary to provide thermal contact with the cooling water, so as to prevent the filaments from overheating during the irradiation. Helium was used due to its low neutron capture cross section. A 2.5 cm diameter, 4.7 cm long water flooded aluminum can containing 25 ampoules was then exposed to an isotropic flux of reactor neutrons, consisting of 98% thermal neutrons (E =25.3 meV) and 2% epithermal neutrons (ranging in energy up to 10 keV), at the Missouri University Research Reactor (MURR) for time periods of 24, 48, 72, and 96 h. The exposures corresponded to fluences of 4.75×10^{18}, 9.50×10^{18}, 1.43×10^{19}, and 1.90×10^{19} cm^{-2} respectively (Table I). Table I also includes estimates of the atomic percentage of boron converted to lithium. The fluences were estimated using a cobalt doped aluminum flux wire. The percent of lithium produced was estimated, under the assumption of a uniform fluence throughout the sample, by the product of the density of ^{10}B, the ^{10}B neutron capture cross section, and the neutron fluence.[19] Post exposure anneals were performed with the samples still sealed within the quartz ampoules for temperatures up to 500 °C in a Lindberg model 55035 Mini-Mite tube furnace. In each case, we annealed an ampoule at a given temperature for a set period of time. Upon removal from the furnace, the ampoules were quenched in air and then opened in order to perform measurements on the individual wires. Each data point (i.e., each fluence/annealing time/annealing temperature) is from a single sample that was annealed only once. In some cases we measured several samples that underwent nominally the same conditions, and this was done either by using different wires within a given ampoule or from annealing additional ampoules under the same profile. In all cases measurements were performed on samples that underwent only a single anneal.

The boron filaments used in this study contain a tungsten boride core. Fast neutrons colliding with ^{182}W atoms, which have a natural abundance of 26.3%, can be absorbed into the nucleus causing the emission of a proton and transforming the tungsten into ^{182}Ta. ^{182}Ta β decays back to ^{182}W, with a half life of 181 days. As a result the filaments were mildly radioactive and required appropriate safety measures in handling.

Powder x-ray diffraction (XRD) measurements were made at room temperature using Cu$K\alpha$ radiation in a Rigaku Miniflex Diffractometer. A silicon standard was used to calibrate each pattern. The experimentally determined Si peak positions were found to be offset from their known values by a constant amount. Within each spectra, the peaks varied about some constant offset and this variation was used to estimate experimental uncertainty in the lattice parameters. Lattice parameters were determined from the position of the (002) and (110) peaks. The dc magnetization measurements and magnetization hysteresis loops were performed in a Quantum Design MPMS-5 SQUID magnetometer. Transport measurements were done using a standard ac four probe technique, with platinum wires attached to the samples with Epotek H20E silver epoxy. In a previous study[25] we note that during the synthesis of the boron filament, the tungsten reacts with B in the gas stream, forming a host of tungsten boride compounds. As a result the core is not a low resistance W wire, but a much more highly resistive alloy of the refractory boride materials W_xB_y that, due to expansion associated with the formation of the MgB_2, is segmented. In addition to the transmutation of some of the W to Ta, the presence of natural boron in the core will lead the presence of defects caused by the transmutation of ^{10}B to ^{7}Li, just as in the MgB_2 wire. Additionally, the cross section of the core is only 2% of the cross section of the wire. We therefore take the measurement of the resistivity to represent the resistivity of the MgB_2. (This assumption is valid as long as the resistivity of the core remains above $\sim$0.5 $\mu\Omega$ cm. Given the nonstoichiometry, radiation damage, transmutation, and segmentation of the core, we feel this is a safe assumption.) Resistivity versus temperature measurements in applied magnetic fields up to 14 T were carried out in a Quantum Design PPMS-14 system and resistivity versus field was measured up to 32.5 T in a dc resistive magnet using a lock-in amplifier technique at the National High Magnetic Field Laboratory in Tallahassee, Florida.

III. FLUENCE AND ANNEALING STUDIES

Normal state and superconducting properties were found to be a function of fluence, annealing time, and annealing temperature. We present the data in the following order: (a) structural studies on as-damaged wires, (b) 24 h anneals at varying temperatures for a fluence of 4.75×10^{18} cm^{-2}, (c) variable time anneals for a fluence of 4.75×10^{18} cm^{-2}, (d) 24 h anneals for all measured fluence levels, and (e) 1000 h anneals on all four fluence levels. With these cuts through the multiparameter, fluence, annealing temperature, annealing time phase space, we can start to describe the effects of neutron damage on MgB_2 samples made with natural boron.

A. Structural studies of as-damaged samples

The x-ray (002) and (110) peaks for an undamaged wire and the entire set of as-damaged samples are plotted in Fig.

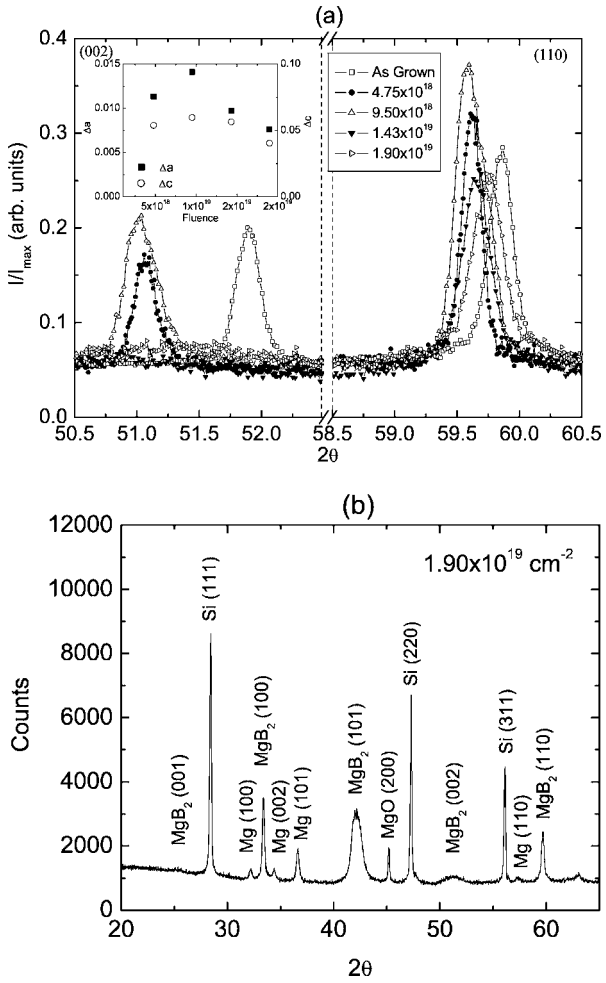

FIG. 1. (a) (002) and (110) x-ray peaks for undamaged, 4.75×10^{18}, 9.50×10^{18}, 1.43×10^{19}, and 1.90×10^{19} cm^{-2}, fluence as-damaged samples. The highest two fluence levels show a broadened (002) peak, indicating a decrease in order along the c axis. The inset shows the relative shift of the a- and c-lattice parameters as a function of the fluence level. (b) The fuller diffraction pattern of the as-damaged 1.90×10^{19} cm^{-2} fluence level sample. On this fuller range the broadened (002) peak is clearly visible.

1(a). The lowest exposure level, 4.75×10^{18} cm^{-2}, shows an anisotropic expansion of the unit cell. The a-lattice parameter increases from 3.0876(5) Å in the undamaged sample to 3.0989(2) Å, an increase of 0.0113(7) Å or 0.37%. The c-lattice parameter increases from 3.5209(7) to 3.5747(2) Å, an increase of 0.0538(9) Å or 1.02%. A similar anisotropic expansion of the unit cell was seen by Karkin *et al.*[15] The authors report lattice parameter increases of $\Delta a=0.0075$ Å or 0.24% and $\Delta c=0.0317$ Å or 0.9% for a fluence of 1×10^{19} cm^{-2} thermal neutrons and 5×10^{18} cm^{-2} fast neutrons. For irradiation of isotopically enriched $Mg^{11}B_2$, little change was seen in the a-lattice parameter up to a fluence level of 10^{17} cm^{-2}.[22] For this fluence level, the authors report a 0.008 Å or 0.23% increase in the c-lattice parameter relative to an undamaged sample. Due to the large differences in Δa and Δc reported for different irradiation conditions, we performed a systematic study of the lattice parameters as a function of the fluence level, annealing temperature, and annealing time for samples all prepared in the same manner.

Relative to the 4.75×10^{18} cm^{-2} fluence level, filaments exposed to a fluence of 9.50×10^{18} cm^{-2} show a further expansion of the unit cell, with the a- and c-lattice parameters reaching 3.1017(7) and 3.5805(10) Å, respectively. The response to further increases in exposure qualitatively changes. For an exposure level of 1.43×10^{19} cm^{-2}, the (002) peak broadens substantially, and the a- and c-lattice parameters contract relative to the samples exposed to the 9.50×10^{18} cm^{-2} fluence level. Increasing the fluence further to 1.90×10^{19} cm^{-2} results in a further contraction of both the a- and c-lattice parameters with the (002)peak remaining broad. The x-ray scan for the as-damaged, 1.90×10^{19} cm^{-2} fluence level sample, from $2\theta=20-65°$ is plotted in Fig. 1(b). The peak widths for the MgB_2 (hk0) peaks are within a factor of 2 of the widths for neighboring Si peaks, whereas the MgB_2 (001) peak is not resolvable and the (002) peak is more than five times as broad as the Si peaks. It should be noted that in pure, undamaged MgB_2 all x-ray peaks have full width at half maximum (FWHM) values comparable to those of the Si standard. For example, the peaks used to determine the lattice parameters in the undamaged wires used in this study, the (002) and (110), had FWHM values of 0.216° and 0.221°, respectively. The neighboring Si peak, the (311) peak that occurs at 56.110° 2θ, had a FWHM of 0.190°.

In the case of a fluence level of 1.90×10^{19} cm^{-2}, the MgB_2 (100) peak, occurring at $2\theta=33.397°$, has a full width at half maximum (FWHM) of 0.216°, in comparison to the FWHM of 0.180° for the Si (111) peak at $2\theta=28.422°$. Similarly, the MgB_2 (110) and Si (311), which occur at 59.686° and 56.110° 2θ, had FWHM values of 0.291° and 0.163°, respectively. In contrast, the MgB_2 (002) peak has a FWHM of 1.335°. The resultant correlation lengths, given by $\Delta 2\theta=\lambda/d\cos(\theta)$, are approximately 4000 Å in the plane and 700 Å along the c direction. The mixed (101) peak has a FWHM of 1.045° and a correlation length near 1000 Å, values intermediate between the two extrema. The two highest fluence levels have resulted in an anisotropic change in the correlation length, with a decrease in long range order between the boron planes. Since the (002) peak has substantially broadened for higher fluence levels, tracking the trend in Δc becomes harder due to the inherent decrease in accurately defining the peak position.

B. 24 hour anneals of samples exposed to a fluence of 4.75×10^{18} cm^{-2}

As-damaged samples showed a suppression of T_c to below 5 K. This is a much larger suppression than seen upon irradiating $Mg^{11}B_2$:[22] the authors report a T_c of 12.2 K for a fluence of 3.9×10^{19} cm^{-2}. Irradiation of MgB_2, i.e. with natural boron, using a fast neutron fluence of 2×10^{18} cm^{-2} gave a T_c of 30.2 K.[17] Thus, damage induced via neutron capture and subsequent alpha decay appears to play a significant role in suppressing superconductivity. To further investigate the effects of uniform irradiation on samples containing natural boron we have performed a systematic study of the normal state and superconducting properties as a function

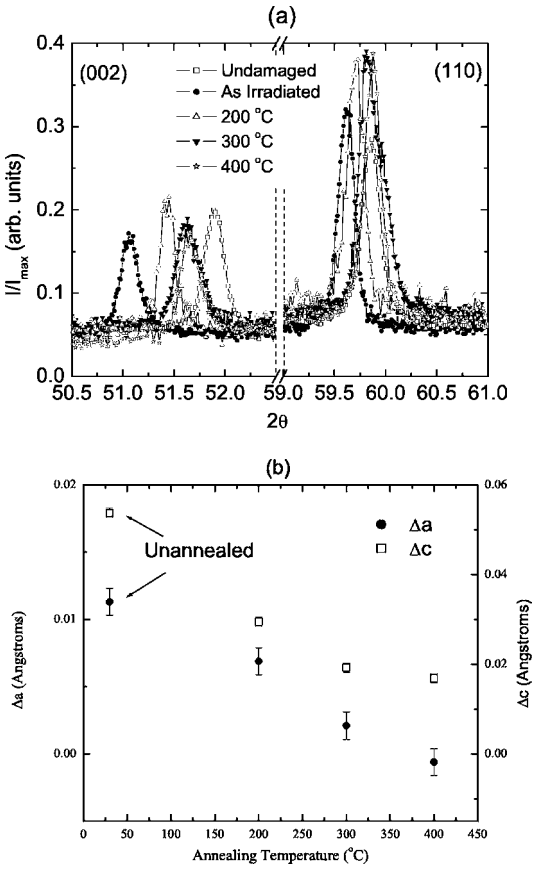

FIG. 2. (a) (002) and (110) x-ray peaks used to determine the *a*- and *c*-lattice parameters for the set of 24 h anneals on samples exposed to a fluence of 4.75×10^{18} cm^{-2}. (b) The evolution of the lattice parameters as a function of annealing temperature. Closed symbols represent Δa and open symbols are Δc.

of the annealing temperature for samples annealed for 24 h.

We annealed a set of wires, exposed to a fluence of 4.75×10^{18} cm^{-2}, for 24 h at 100 °C, 150 °C, 200 °C, 300 °C, 400 °C, and 500 °C. X-ray measurements indicate the initial expansion of the unit cell could be systematically reversed by subsequent annealing (Fig. 2), with the Δa and Δc values decreasing with increasing annealing temperature (Fig. 2(b)). The *a*-lattice parameters is completely restored after annealing at 400 °C, whereas the *c*-lattice parameter appears to be saturating at a value near 0.6% larger than that of the undamaged sample.

The superconducting transition temperatures were determined using a 1% screening criteria in zero field cooled dc magnetization measurements (Fig. 3(a)) and an onset criteria in resistivity versus temperature measurements (Fig. 3(b)). The magnetic transitions for the entire set are fairly sharp, typically achieving 95% of the saturated value 2.5 K below the 1% criteria used for T_c. This suggests a relatively homogeneous damaging of the sample. We were unable to obtain reliable transport measurements on as-damaged as well as the 100 °C annealed samples due to the 120 °C temperature required to cure the silver epoxy contacts. The 30 min 120 °C cure of the epoxy, as well as the possible exotherm associated with the epoxy curing, placed the sample into a poorly defined annealed state. As shown in Figs. 3(a) and 3(b), superconductivity is restored by the annealing process. ΔT_c, defined as the difference between the undamaged T_c and that of the annealed sample, monotonically approaches zero as the annealing temperature is increased (Fig. 4).

The zero field temperature dependent resistivity data are plotted in Fig. 3(b). The sample annealed at 150 °C has a low temperature normal state resistivity slightly above 6 $\mu\Omega$ cm, which is an order of magnitude larger than the undamaged value of 0.2 $\mu\Omega$ cm. After annealing at a temperature of 200 °C, ρ increases by another fourfold. Further increases in the annealing temperature result in a monotonic decrease of the normal state resistivity, to 1.6 $\mu\Omega$ cm at an annealing temperature of 500 °C. Although we were able to perform a measurement on only a single sample, this increase in ρ at 200 °C is thought to be a real effect, as it also manifests itself in normalized $\rho/\rho(300\ \mathrm{K})$ plots, indicating it is not associated with a pathologic geometric problem such as cracks. Additionally, undamaged samples consistently showed T_c values near 39 K and normal state resistivities in the 0.2–0.4 $\mu\Omega$ cm range, values in agreement with previously published results,[24,26] suggesting that the effect is the result of the irradiation and post-exposure annealing process. Such an anomalous increase in resistivity as a function of annealing temperature was also observed in the case of neutron irradiation on carbon doped MgB_2 wire segments.[27] The initial annealing may result in a change in the defect structure. For example, vacancies do not necessarily immediately recombine with interstitials to eliminate defects. Vacancies can initially cluster together to form higher order defects, which can be relatively stable.[14] Thus, the initial increase in resistivity may result from a reorganization of defects into higher order clusters, which may enhance scattering.

Insight into the nature of the defects can be obtained by tracking changes in the parameter $\Delta\rho=\rho(300\ \mathrm{K})-\rho(40\ \mathrm{K})$. Figure 3(d) plots $\Delta\rho$ as a function of the transition temperature. $\Delta\rho$ decreases monotonically as a function of the transition temperature. This result is in contrast to the results of He ion irradiation on MgB_2 thin films,[28] but in agreement with the predictions of Mazin *et al.*,[29] who claimed that as a material is driven into the dirty limit, the conductivity in the pi band decreases, causing normal state electric transport to switch from the pi to the sigma band. Indeed, for the extreme clean and extreme dirty limits they obtain values ranging from near 10 to near 35 $\mu\Omega$ cm, respectively, consistent with our experimental observations of 6 and 35 $\mu\Omega$ cm.

An alternate framework for understanding this monotonic change in $\Delta\rho$ is to recall that the sample is polygrain with random orientation of the crystallites. Given that the electrical resistivity of MgB_2 is anisotropic to start with, combined with the fact that damage appears to more aggressively affect the *c* axis periodicity, it is possible that for lower T_c values an increasing number of grain orientations will present high resitivity paths to the current. This will effectively reduce the cross sectional area of the wire sample. This would result in a similar behavior to what has been found for samples that have either poor connectivity or gross impurities on the grain boundaries.[30]

The upper critical field was determined using an onset criteria in resistivity versus temperature in applied fields up to 14 T (a representative set is shown in Fig. 5(a)), and, in

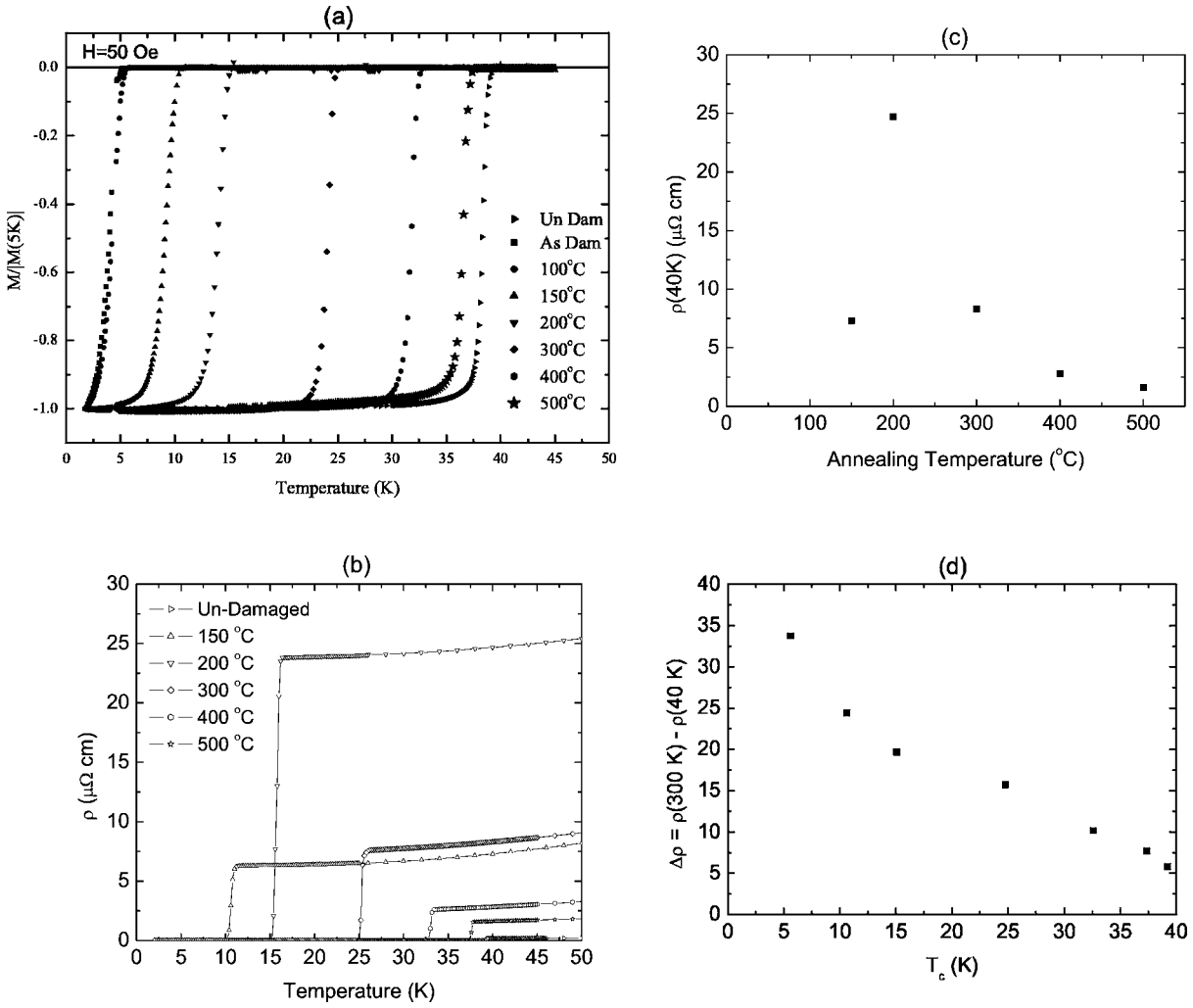

FIG. 3. (a) Normalized magnetization and (b) resistivity curves for the set of 24 h anneals on samples exposed to a fluence of 4.75×10^{18} cm^{-2}. (c) The normal state resistivity at 40 K. The resistivity shows a sharp increase at an annealing temperature of 200 °C, then decreases approximately exponentially as a function of annealing temperature. (d) $\Delta\rho$ versus transition temperature.

the case of the 500 °C anneal, resistance versus field sweeps up to 32.5 T (Fig. 5(b)). The upper critical field curves nest, forming a sort of Russian doll pattern, with $H_{c2}(T=0)$ approximately scaling with T_c (Fig. 6). The curves for samples annealed at temperatures up to 200 °C do not show any positive curvature near T_c and are qualitatively similar to single gap superconductors with Werthamer, Helfand, and Hohenberg (WHH)[32] like behavior. Experimentally determined H_{c2}(T=0) values for the 150 °C, 200 °C, and 300 °C anneals are 2.9, 4.7, and 7.3 T respectively. Using the formula $H_{c2}(T=0)=0.69T_c\, dH_{c2}/dT$, we obtain estimates of 2.9, 4.3, and 5.9 T. Thus, whereas only in the cases of the 150 °C and 200 °C anneals we can fit H_{c2}(T) with WHH behavior, the deviations increase with the annealing temperature, suggesting that the bands may become fully mixed only when T_c is suppressed to near 10 K. Single gap behavior has been inferred from specific heat measurements on irradiated samples containing isotopically enriched ^{11}B that had T_c near 11 K.[33] The 300 °C, 400 °C, and 500 °C anneals exhibit positive curvature near T_c that is similar to what is found in pure MgB_2. The 500 °C anneal data show that either the undamaged $H_{c2}(T)$ is restored or that there a slight increase in $H_{c2}(T=0)$, rising from approximately 16 T in the undamaged case to near 18 T.

This behavior in H_{c2} differs from other types of neutron damaging studies. For the case of irradiating isotopically enriched $Mg^{11}B_2$. Putti *et al.* found a fairly substantial increase in H_{c2} values when T_c was in the 36–38 K range.[20] For a sample with T_c=36.1 K, they report $H_{c2}(T=12\text{ K})$ of 20.3 T. For unshielded irradiation of MgB_2 containing natural boron, Eisterer *et al.*, reported that, relative to an undamaged sample with a T_c just below 38 K, a sample with a suppressed T_c of approximately 36 K had a near doubling of the slope dH_{c2}/dT in the linear regime above 2 T.[16] In both of these cases the fluences used were an order of magnitude lower than in our experiment, and no post exposure annealing was performed.

Figure 7 presents the critical current densities for the series of 24 h anneals at 5 and 20 K, as determined by the Bean critical state model[34] from magnetic hysteresis loops. At both 5 and 20 K, J_c is suppressed for samples annealed at 300 °C and below, presumably due to the larger reduced

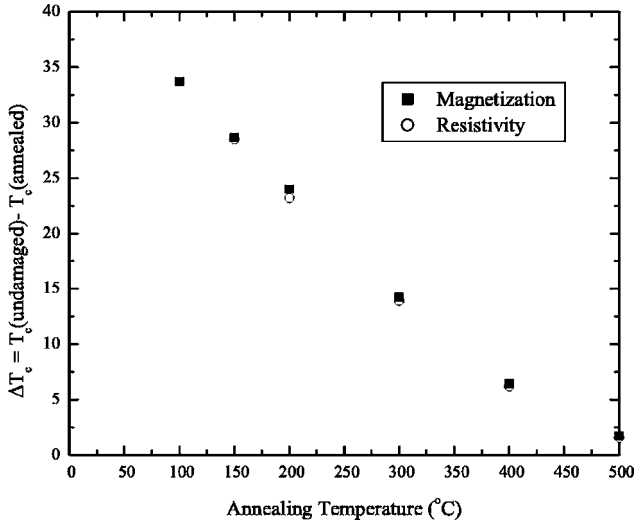

FIG. 4. Restoration of superconductivity by post exposure annealing for samples exposed to a fluence of 4.75×10^{18} cm^{-2} and subsequently annealed for 24 h at various temperatures. Transition temperatures were determined using a 1% screening criteria in magnetization and an onset criteria in resistivity. Annealing at 500 °C yields a T_c near 37.5 K, less than 2 K below that of the undamaged sample.

temperature (T/T_c) of the measurements. In field J_c values become enhanced at both 5 and 20 K for the 400 °C and 500 °C anneals, and show a slight fishtail or second peak behavior. This is believed to be the first time such behavior has been observed in polycrystalline samples. The fishtail effect has been seen in the fast neutron irradiation of MgB_2 single crystals.[21] The authors report a second peak in the magnetization hysteresis loops for $H\perp ab$, which became more pronounced with increasing fluence up to 4 V $\times10^{17}$ cm^{-2}. No second peak was observed for $H||ab$. Low level thermal neutron fluence, of order 10^{14}–10^{15} cm^{-2}, of polycrystalline MgB_2 showed an enhancement in flux pinning, but no second peak or fishtail behavior.[17] The infield enhancement of J_c for the sample annealed at 500 °C pushes the point at which J_c crosses 10^4 A/cm^2 at 20 K out to near 1.5 T. This increase in field roughly doubles the crossing point of the undamaged wire, but falls well below the best reports in the literature of 10^4 A/cm^2 at near 5 T reported for ten 10 weight percent addition of SiC to MgB_2.[37]

Other authors have analyzed critical current densities in neutron irradiated samples using a percolative model that considers, as free parameters, the upper critical field, the absolute value of the critical current density, the anisotropy of the upper critical field, and the percolation threshold.[31,35,36] In Ref. 36 the authors extend the model to include different contributions from grain boundary and precipitate pinning. The model yields extremely good fits to the data, from which the authors conclude that the anisotropy of H_{c2} heavily influences the field in which the material can carry large amounts of current[31,35] and defects introduced by the irradiation process are responsible for the enhancement of the pinning strength.[36] It is worth noting that these reports do not show the significant change in $J_c(0)$ that we observe (Fig. 7). Presumably two effects are causing the increase as a function of

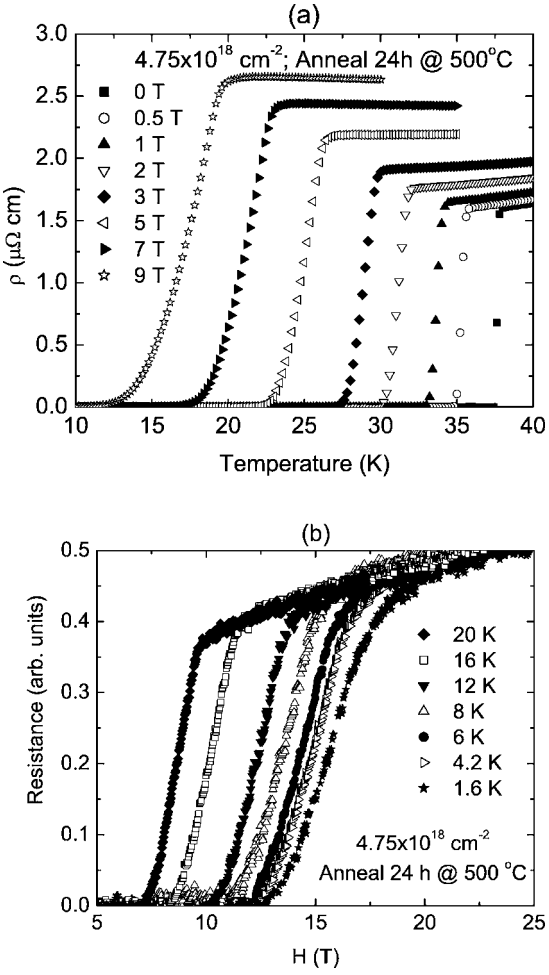

FIG. 5. Transport measurements to determine the upper critical field. (a) Resistivity versus temperature and (b) resistance versus field. H_{c2} values were determined using the onset criteria in both measurements.

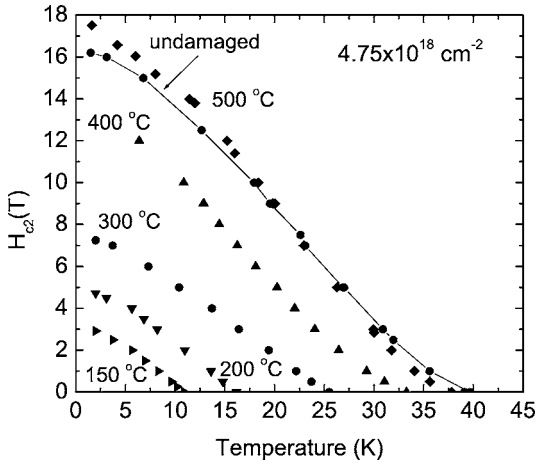

FIG. 6. Upper critical field curves for undamaged as well as for samples exposed to a fluence of 4.75×10^{18} cm^{-2} and annealed at 150 °C, 200 °C, 300 °C, 400 °C, and 500 °C for 24 h.

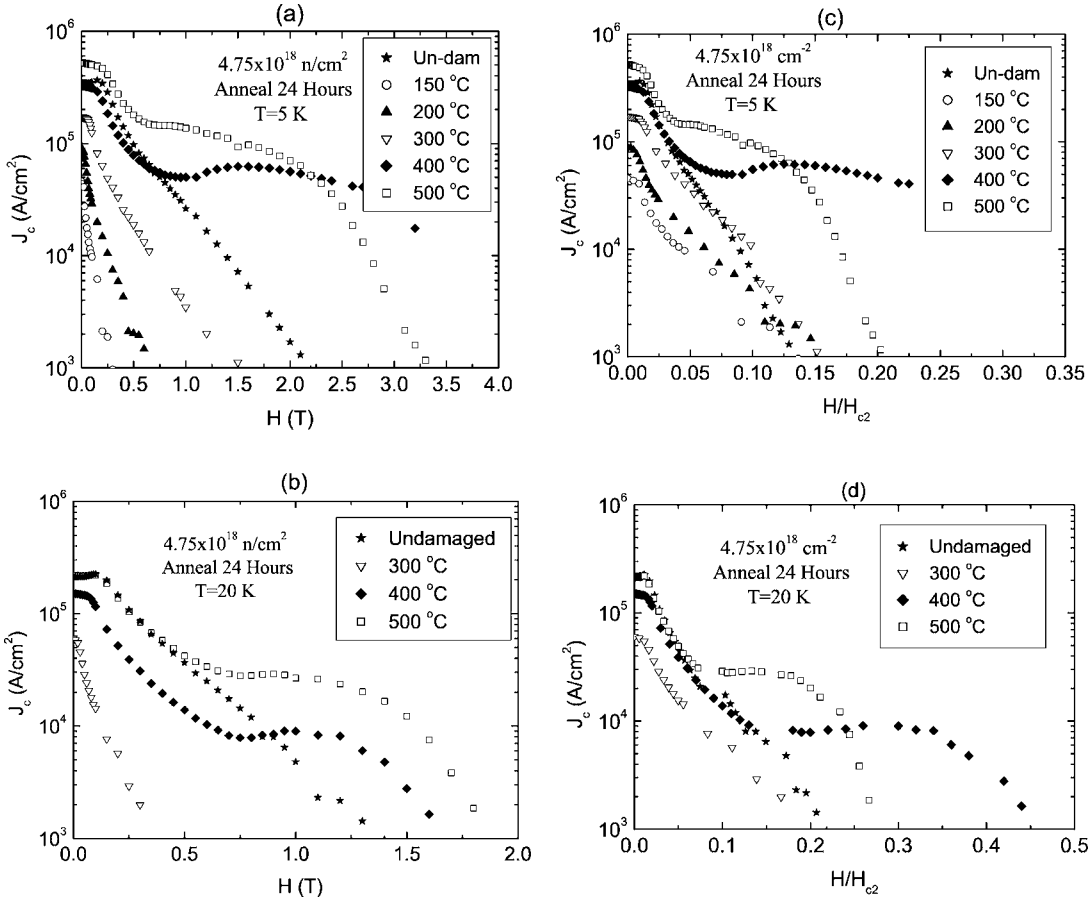

FIG. 7. Critical current densities as a function of field at (a) 5 K and (b) 20 K for samples irradiated with a fluence of 4.75×10^{18} cm^{-2} and subsequently annealed for 24 h at various temperatures. (c) and (d) plot J_c as a function of the reduced field H/H_{c2}.

annealing temperature and hence T_c. In using the percolation model, each of the authors kept the percolation threshold fixed in the 0.2–0.3 range. If we are observing large changes in the connectivity in our samples as a function of annealing temperature, as inferred from the $\Delta\rho$ data, then the initial decrease in $J_c(0)$, as observed in the low temperature anneals, is the result of the formation of weak links that limit the overall critical current density. As the annealing temperature is increased the connectivity between grains is improved, thereby returning $J_c(0)$ toward the undamaged value. In the case of the 500 °C anneal, $J_c(0)$ exceeds that of the undamaged sample, suggesting that the defects that remain following post-exposure annealing act aseffective pinning sites. If defects caused by irradiation are 0.1–10 nm in size, as reported in Ref. 31, then following the annealing process, many of the defects should be of order the coherence length,[39] making them effective flux pinning centers.

A plot of J_c as a function of reduced field (H/H_{c2}) shows that for the higher temperature anneals, the fraction of H_{c2} in which samples can maintain in excess of 10^3 A/cm^2 is greatly enhanced (Figs. 7(c) and 7(d)). Such enhancement is consistent with an increase in the strength of defect pinning.[36] That the low temperature anneals all show J_c dropping below 10^3 A/cm^2 at similar reduced field values suggests that the defects are ineffective in enhancing critical current densities in highly disordered samples. This could be the result of, for example, the overlap of defects, making them too large to be effective flux pinning sites.

C. Variable time anneals on samples exposed to a fluence of 4.75×10^{18} cm^{-2}

The annealing time for the set of 4.75×10^{18} cm^{-2} fluence samples was varied to further probe the characteristics of damage induced by neutron irradiation. An extensive set of anneals was carried out at 300 °C, consisting of 1/3, 1, 3, 6, 24, 96, and 1000 h. For annealing temperatures of 200 °C and 400 °C, measurements were done on 1, 24, and 96 h anneals. Two anneals were performed at 500 °C: one for 24 h and the other for 1000 h.

The magnetic transitions for the entire set of samples annealed at 300 °C are shown in Fig. 8. Annealing at this temperature for only 0.33 h raised T_c from below 5 K to slightly above 19 K. Therefore, the defects causing the suppression of superconductivity must have a fairly low activation energy. For defects that can be annealed by a single activated process with a constant activation energy, the rate of change of the defect concentration is given by[14]

$$dn/dt = -F(n)K_0 e^{-E_a/k_B T}, \tag{2}$$

where n is the defect concentration, $F(n)$ is some continuous function of n, K_0 is a constant, E_a is the activation energy, k_B

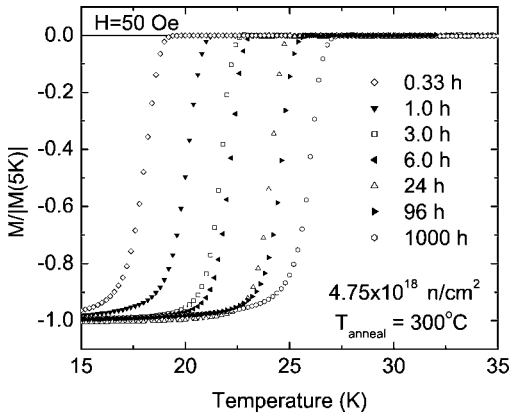

FIG. 8. Normalized magnetization curves for a fluence level of 4.75×10^{18} cm^{-2} annealed at 300 °C for 1/3, 1, 3, 6, 24, 96, and 1000 h.

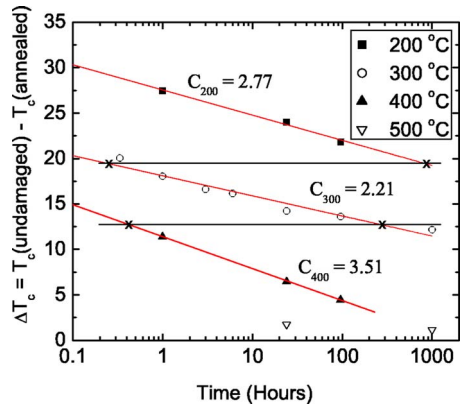

FIG. 9. (Color online) Semi-log plot of the change of the superconducting transition temperature as a function of annealing time at various annealing temperatures. All samples shown were exposed to a fluence level of 4.75×10^{18} cm^{-2}. Using a linear fit over up to three decades yields non-systematic values in the rate constants for the 200 °C, 300 °C and 400 °C annealing temperatures. The activation energy is estimated using the cross cut procedure on extrapolations of these fits to the data (comparison points are given by the x symbols). By comparing points with identical ΔT_c values, through equation 3 we obtain estimates of E_a=1.90 eV and 2.15 eV (see equation 4).

is Boltzmann's constant, and T is the temperature. If we assume random diffusion, then $F(n)=n$, and the defect concentration decreases exponentially with time:

$$n = n_0 e^{-Ct}, \tag{3}$$

where n_0 is the initial defect concentration, $C=K_0 e^{E_a/k_B T}$ is a rate constant, and t is time.

While ρ_0 can be taken as one measure of the defect concentration, we have already shown nonmonotonic behavior in ρ_0 as a result of the annealing process. Another variable that can be used to defect concentration is T_c, which systematically varies with both annealing temperature and annealing time. We therefore take ΔT_c as a measure of the defect concentration, although it should be reiterated that the nature of the defects may be changing as we increase the annealing temperature and time. Such linearity is not uncommon and can be related to Abrikosov-Gorkov-like theory of pair breaking in anisotropic superconductors.[40] It should be noted, though, that we do this simply in an attempt to extract an approximate value of the activation energy.

We see an exponential decay behavior in ΔT_c for samples annealed at 200 °C, 300 °C, and 400 °C (Fig. 9). Since we only have two samples annealed at 500 °C, which are longer time anneals and thus presumably would fall farther out on an exponential tail, we cannot extract a meaninful value from an exponential fit of these data. For samples that do show an exponential behavior in the decrease of ΔT_c (and by presumption) the defect density as a function of annealing time, the activation energy, assuming a single activation process, can be determined by the so-called cross-cut procedure.[14] This involves comparing the annealing time for which different temperature anneals reached the same defect density, i.e., ΔT_c. If a ΔT_c is reached by annealing at a temperature T_1 for a time t_1 and by annealing at a temperature T_2 for a time t_2, then the activation energy is related to these quantities by

$$\ln\frac{t_1}{t_2} = \frac{E_a}{k_B}\left(\frac{1}{T_1} - \frac{1}{T_2}\right). \tag{4}$$

Unfortunately, no overlap region in T_c exists for our set of data. To achieve an overlap region in the experimental data we would need to shorten the annealing times to below 0.33 h or extend them to well beyond 1000 h. Short time anneals, less than 0.33 h, are not feasible, as we would be unable to ensure thermal equilibrium of the samples within the furnace for such a short time. Extending the annealing an additional order of magnitude, to 10^4 h, is simply not practical. We can still estimate the activation energy by extrapolating the ΔT_c curves at each temperature to shorter and longer times so as to create overlap regions (Fig. 9). Calculating E_a from the overlap between the 200 °C and 300 °C curves and between the 300 °C and 400 °C curves yields values of 1.90 and 2.15 eV, respectively.

An alternative approach to determining the activation energy is to use the ratio of slopes method.[38] Experimentally, a set of samples is annealed isothermally for different times at a temperature T_1 and an identical set of samples is annealed at a different temperature T_2. The differing temperatures result in different time evolution of ΔT_c, and hence, different slopes, $d\Delta T_c/dt$. The ratio of the slopes for the two different temperatures at the point where both annealing temperatures have yielded the same ΔT_c is related to the activation energy by

$$\frac{d\Delta T_{c1}}{dt_1}\Big/\frac{d\Delta T_{c2}}{dt_2} = \exp\left[\frac{E_a}{k_B}\left(\frac{1}{T_1} - \frac{1}{T_2}\right)\right], \tag{5}$$

where the subscripts 1 and 2 refer to temperatures T_1 and T_2. By comparing the slopes from the 200 °C and 300 °C anneals and those from the 300 °C and 400 °C anneals, we obtain estimates of 1.07 and 1.63 eV, respectively. It should be noted that, while these estimates were made using real data, rather than extrapolations as in the previous calculation, there is an inherent inaccuracy in such a calculation due to the lack of a true overlap in ΔT_c. Additionally, the low den-

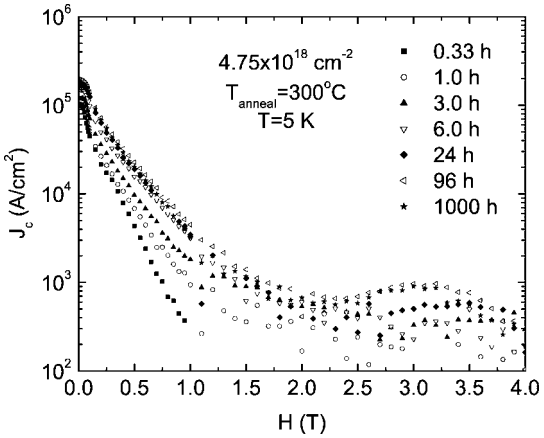

FIG. 10. J_c curves (inferred from magnetization data) for the set of 4.75×10^{18} cm^{-2} fluence samples annealed at 300 °C for various times.

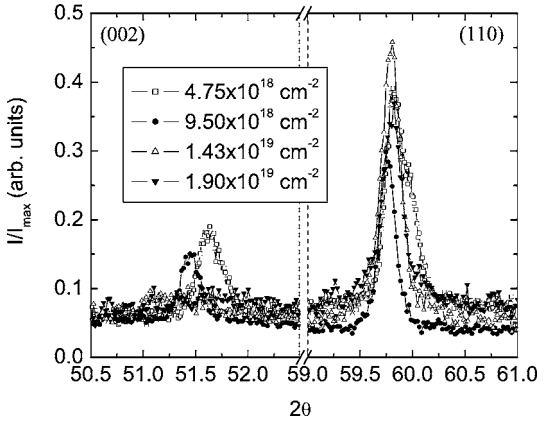

FIG. 11. (002) and (110) x-ray peaks for all four exposure levels annealed at 300 °C for 24 h. The highest two levels continue to show a substantially broadened (002) peaks, indicating a degradation of long range order along the c direction.

sity of data points limits our ability to accurately determine the linear slope from the ΔT_c versus time curves, where ΔT_c tends to decay exponentially.

Depending on the calculation method and dataset used, we obtain activation energies ranging from 1.07 to 2.15 eV. It is likely that some of the variation is real, as, in these heavily damaged samples, there exist both point defects and defect complexes. The annealing of point defects is expected to have a lower activation energy than the dissolving of the defect complexes. While we cannot assign definitive values for the activation energies of these two processes, merely stating a single activation energy hides some of the rich complexity underlying the annealing process in these heavily damaged samples. It should be noted that the activation energies in these neutron-irradiated MgB_2 samples are the same order of magnitude as those for annealing quenched in defects out of gold.[38] That our samples yielded a relatively small spread in activation energies and were comparable in magnitude to values associated with the annealing of simple defects in other metals suggests that the defects within the neutron-irradiated MgB_2 samples are being annealed by single activation processes.

For the set of wires annealed at 300 °C, critical current densities at $T=5$ K and low fields approximately scale with annealing time and, hence, T_c (Fig. 10). The field at which J_c drops below 10^4 A/cm^2 increases by approximately a factor of 2 when the annealing time is increased from 1 to 24 h. Extending the annealing time further to 1000 h has little effect on low field J_c values. For annealing times of 6 h and shorter (for the sake of clarity, data for 1/3, 3, and 6 h are not shown), J_c was found to monotonically decrease as a function of the applied field. After a 24 h anneal, J_c begins to flatten above 3 T at a value of approximately 500 A/cm^2. Extending the annealing time to 96 and 1000 h results in the emergence of a clear second peak at an applied field slightly above 3 T. The curves for the 96 and 1000 h anneal are virtually identical and reflect the small 1.5 K or 6% increase in T_c resulting from the order of magnitude longer annealing time.

D. Variable fluence levels, 24 h anneal

We annealed samples from each of the damaged levels for 24 h at 200 °C, 300 °C, 400 °C, and 500 °C. The (002) and (110) x-ray peaks for samples of all four damage levels annealed at 300 °C for 24 h are given in Fig. 11. Annealing at 300 °C for 24 h did not restore long range order along the c axis in the samples exposed to the two highest fluence levels of 1.43×10^{19} and 1.90×10^{19} cm^{-2}. For these 24 h anneals, up to an annealing temperature of 400 °C, the (002) peak maintains a FWHM above 1 °, which corresponds to a structural coherence length of approximately1000 Å (Fig. 12). Using $H_{c2}(T=0)$ to determine the superconducting coherence length, one obtains for pure MgB_2 a superconducting coherence length near 50 Å.[39] Measurements on the coherence

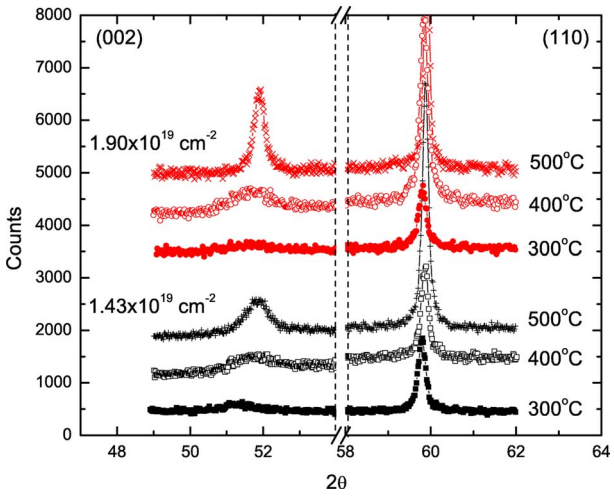

FIG. 12. (Color online) Evolution of the (002) and (110) x-ray peaks for the 1.43×10^{19} and 1.90×10^{19} cm^{-2} exposure levels annealed for 24 h with the annealing temperature increasing from 300 °C to 500 °C. In both cases, the (002) attains a FWHM less than 1 ° 2θ only after the annealing temperature reaches 500 °C. Note: intermediate temperature anneals at 400 °C were performed for longer times to show the persistence of the broadening for $T \leqslant 400$ °C.

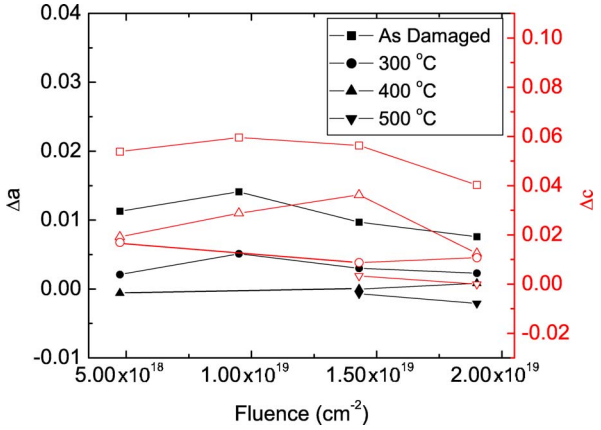

FIG. 13. (Color online) Calculated lattice parameter shifts for all four damage levels annealed at temperatures up to 500 °C. Closed symbols represent Δa, and open symbols are Δc. Lines serve as guides to the eye.

length within the π band only yield a larger value of approximately 500 Å.[41] While there is a shorter range structural order along the c direction in these heavily irradiated samples, the structural coherence length is still at least a factor of 2 larger than the superconducting coherence length, regardless of the estimate of the superconducting coherence length used. It is therefore not unexpected that superconductivity exists in samples with degraded long range order. Only after the temperature reaches 500 °C does the correlation length along the c direction exceed 1000 Å (Fig. 12). The relative shift of the a- and c-lattice parameters for the various heat treatments is plotted in Fig. 13.

Magnetization measurements were performed on all of the annealed samples (Fig. 14(a)). It should be noted that for the fluences greater than 4.75×10^{19} cm^{-2}, as damaged samples showed no signs of superconductivity down to 2 K. A summary of the transition temperatures for each of the annealed samples, given in terms of ΔT_c, is plotted in Fig. 14(b). In general terms, the higher fluence levels lead to lower superconducting transition temperatures for a given temperature post-exposure anneal. For a given fluence level, higher annealing temperatures yield higher T_c values. That is, the samples exposed to higher fluence levels behave in a qualitatively similar manner to the lowest level, but the added exposure leads to increased defect densities that manifest themselves in terms of lower transition temperatures for a given annealing profile.

E. Long time annealing studies

The conversion of ^{10}B to ^{7}Li through neutron absorption and subsequent alpha decay introduces the possibility of observing the effects of lithium doping MgB_2. In order to distinguish the effects of Li doping from those associated with structural defects introduced through inelastic collisions between neutrons and the underlying lattice, it is necessary to minimize the density of these defects. As shown, by annealing for long times at high temperatures, the number of structural defects can be systematically reduced. Since Li cannot be annealed away, the resultant superconducting and normal

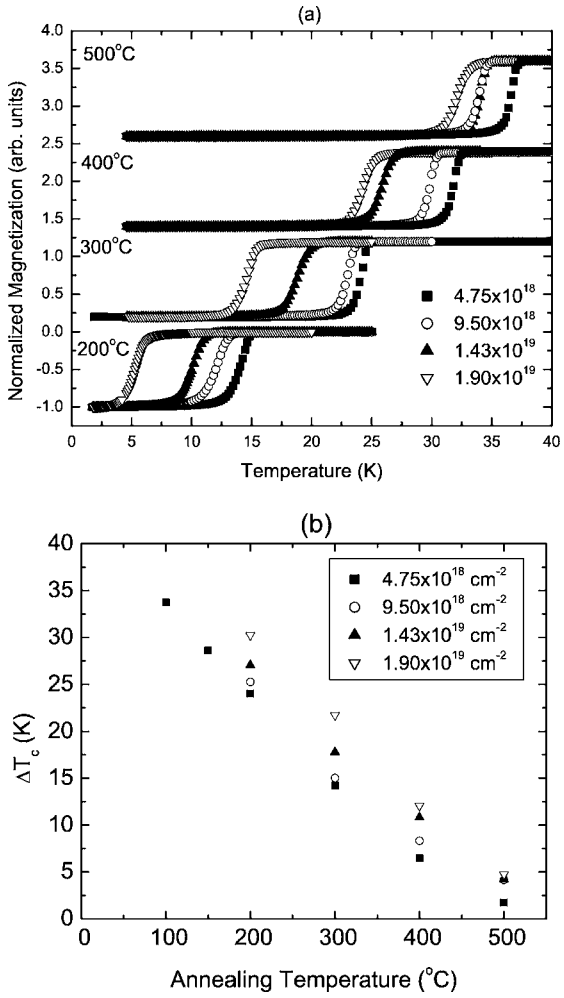

FIG. 14. (a) Normalized magnetic transitions as a function of annealing temperature and fluence level for all four damage levels. The time for each anneal was 24 h. The curves are normalized to a full screening value of −1. The set of curves for each successive annealing temperature is shifted upward by 1.2 units for ease of reading. (b) ΔT_c values, as determined by a 1% screening criteria, as a function of annealing temperature and fluence level.

state properties should increasingly reflect the effects of Li doping. The density of Li atoms produced through the transmutation of boron can be estimated from the formula[19]

$$n_{\mathrm{Li}} = n_{\mathrm{B}} s f, \tag{6}$$

where n_{Li} is the density of Li atoms, n_{B} is the density of B atoms, s is the absorption cross section, and f is the fluence level. Computing the corresponding atomic percentages yields an increase from 0.37% to 1.48% as the fluence in increased from 4.75×10^{18} cm^{-2} to 1.90×10^{19} cm^{-2} (Table I).

We therefore annealed all four of the damage levels for 1000 h at 500 °C. Normalized magnetization curves for this series are plotted in Fig. 15(a). In each case the transition temperatures have increased relative to samples annealed at 500 °C for 24 h, as can be seen by plotting ΔT_c versus time

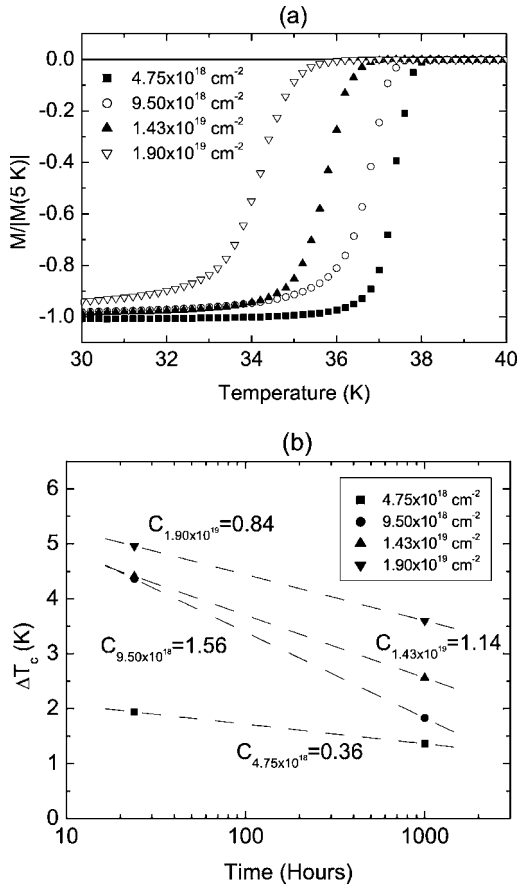

FIG. 15. (a) Normalized magnetic transitions for all four fluence levels annealed at 500 °C for 1000 h. (b) ΔT_c for samples annealed at 500 °C for 24 and 1000 h. For each of the four fluence levels, extending the annealing time results in a further recovery of T_c toward that of the undamaged sample. Rate constants, C, are determined by a linear fit of the semilog plot assuming ΔT_c follows a decaying exponential as a function of time.

(Fig. 15(b)). Using a linear fit on the semilog plot, the resultant slopes are much lower than was seen for the 4.75×10^{18} cm^{-2} fluence level samples annealed for various times at 200 °C, 300 °C, and 400 °C (Fig. 9), indicating that ΔT_c is beginning to saturate above 24 h. Since we do not have any intermediate time points, we cannot determine if we have achieved fully saturated ΔT_c values at 1000 h, but we can take the 1000 h anneals at 500 °C as an upper limit on the effects of lithium doping.

Transport measurements were performed in order to determine the normal state resistivity and temperature dependence of H_{c2} for these samples. We were unable to contact the samples exposed to the two highest dose levels. The normal state resistivity (T=40 K) for the sample exposed to a fluence of 4.75×10^{18} cm^{-2} and annealed for 1000 h was approximately 5.3 $\mu\Omega$ cm, which is more than three times the 1.6 $\mu\Omega$ cm measured on the sample annealed for 24 h. The 1000 h anneal sample also had a lower residual resistivity ratio (RRR), 3.3 vs 5.9, indicating that the increase in ρ_0 is not merely an artifact associated with possible geometric effects (cracks within the sample). The 9.50×10^{18} cm^{-2} fluence level sample, which was annealed for 1000 h, had a

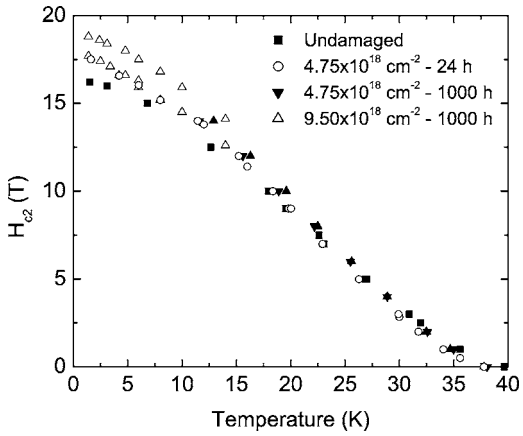

FIG. 16. H_{c2} curves for the 4.75×10^{18} and 9.50×10^{18} cm^{-2} fluence levels annealed for 1000 h at 500 °C. Two sets of data for the low temperature H_{c2} values of the samples exposed to a fluence of 9.50×10^{18} cm^{-2} are shown. Both damage levels show a possible enhancement relative to the undamaged sample, but there is some spread in the data as illustrated by the two 9.50×10^{18} cm^{-2} fluence level samples shown.

normal state resistivity of 6.6 $\mu\Omega$ cm and RRR=5.0. Karkin *et al.* saw increases in ρ for annealing temperatures above 300 °C, which they attributed to changes in intergrain transport.[15] It is possible that by annealing at an elevated temperature for 1000 h we have degraded the intergrain connectivity in some fashion, leading to the observed increases in resistivity.

The temperature dependence of H_{c2} is plotted in Fig. 16. It was found that for the 4.75×10^{18} cm^{-2} fluence level H_{c2}(T), data for a 1000 h anneal sample was comparable to that of the 24 h anneal sample, both showing possible, slight enhancement relative to the pure sample. In the case of the 1000 h anneal on the 9.50×10^{18} cm^{-2} fluence level, H_{c2} had some spread in the data, but extrapolated to 18–19 T at zero Kelvin. The upper critical fields of the two lowest fluence levels annealed at 500 °C for 1000 h appear to be similar, with slight differences arising due to inherent sample to sample variation.

IV. DISCUSSION

The initial irradiation of MgB_2 wire segments results in an increase in the size of the unit cell and suppression of the superconducting transition temperature. Post exposure annealing tends to return both the lattice parameters and T_c toward their undamaged values. If the superconducting properties of the neutron-irradiated samples were purely a result of changes in the unit cell dimensions, correlations should exist between the superconducting properties of neutron-irradiated MgB_2 and pure MgB_2 placed under external pressure. Since an expansion is qualitatively analogous to an effective negative pressure, one would anticipate the changes in T_c be an extension to negative pressure of the results attained for the application of positive pressure. Application of external pressure has been shown to compress the unit cell and suppress T_c.[42] Thin films grown epitaxially on (0001)

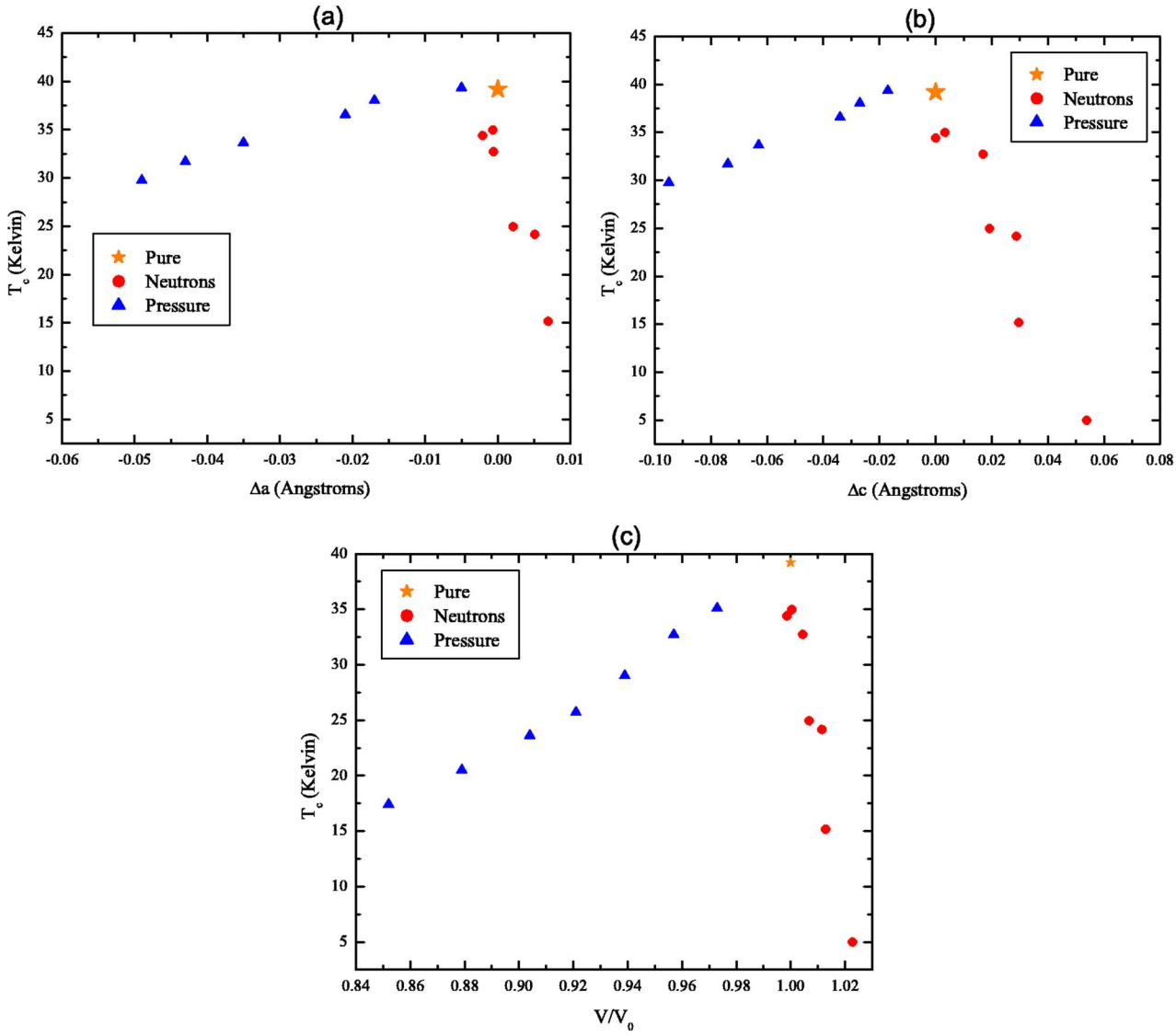

FIG. 17. (Color online) A comparison of the different development of T_c with (a) Δa, (b) Δc, and (c) unit cell volume for neutron-irradiated MgB_2 and MgB_2 under external pressure. Pressure data are recreated from Ref. 42.

sapphire substrates exhibited an enhanced T_c above 41 K that was attributed to tensile strain.[43] In the case of neutron-irradiated MgB_2, the expansion of the lattice parameters coincides with a decrease in T_c and the evolution of T_c as a function of Δa, Δc, and V/V_0 behaves differently than MgB_2 under pressure (Fig. 17). In the case of externally applied pressure, it is believed that the changes in the frequency of the E_{2g} phonon mode are responsible for the suppression of T_c.[42,44] With such dramatically different behavior between the neutron irradiation and pressure results, it is clear that the changes in T_c cannot simply be linked to changes in the unit cell volume.

In addition to the structural changes, neutron irradiation also introduces a chemical impurity into the system through the ^{10}B neutron capture and subsequent alpha decay to ^{7}Li. The amount of lithium produced in this manner is, however, quite small, and for all but the 1000 h anneals at 500 °C, we cannot sort the possible effects of such from the effects of the structural perturbations. The atomic percentage of B converted to Li through nuclear processes for all four exposure levels is estimated to be on the order of 1% (Table I). Therefore, for lower temperature and/or shorter time anneals, the effects of Li production are presumably insignificant next to the changes resulting from structural damage caused by inelastic collisions between the fast neutrons, emitted alpha particles, and recoiled ^{7}Li atoms and the underlying lattice. It is worth noting, though, that whereas low level Li substitution for Mg was proposed as a possible route to increasing T_c,[45] our data show suppressed T_c values for our 1000 h annealed samples. This does not preclude the possibility that Li substitution could, under other circumstances, raise T_c, but it certainly does not support it. It should be noted though that this form of lithium doping is far from the ideal one. In the case of transmutation of $^{10}B$the resulting sample is $MgLi_xB_{2-x}$ with boron vacancies and no clear site for the lithium. The more desirable form of lithium doping is

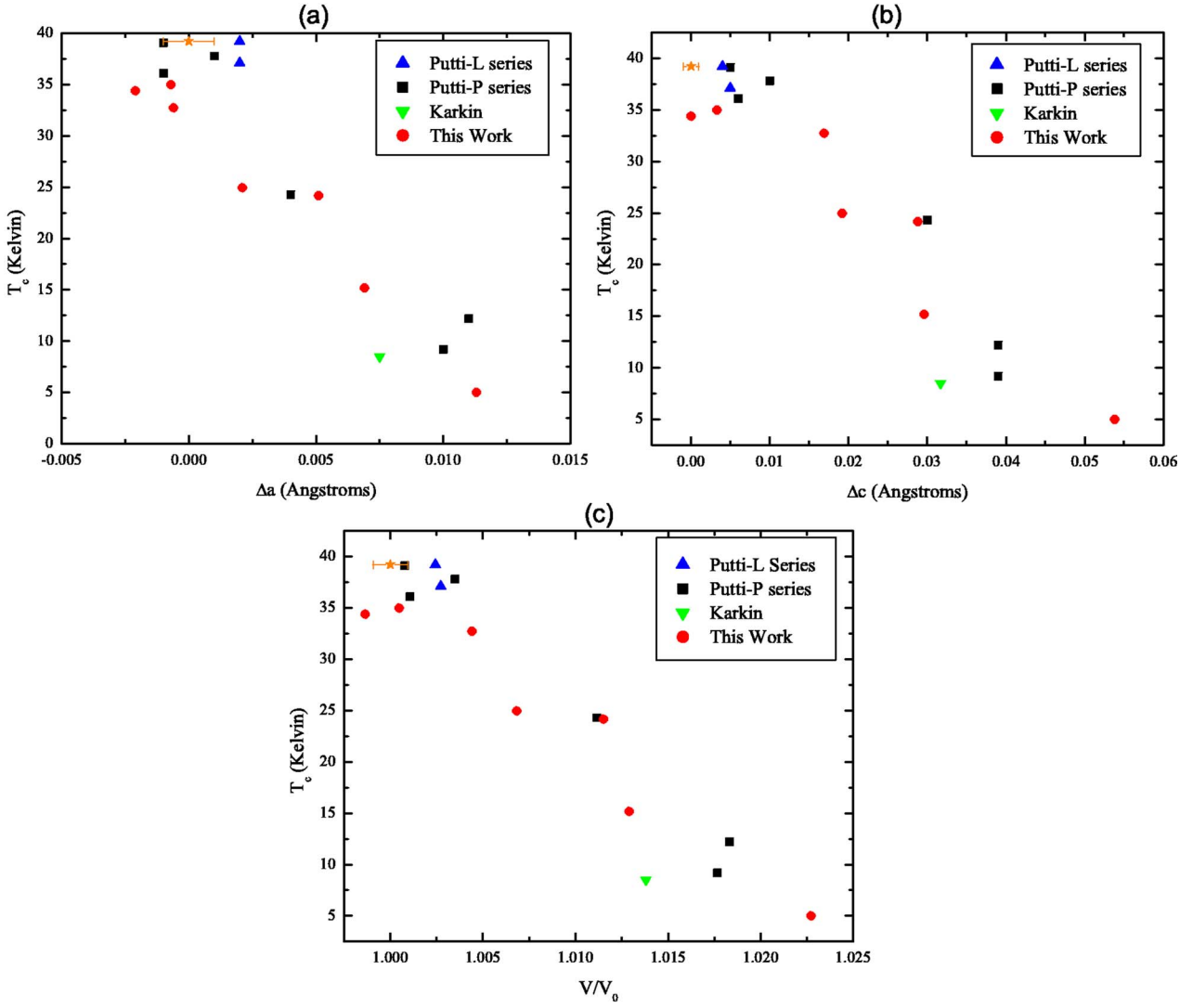

FIG. 18. (Color online) A comparison of the different development of T_c with (a) Δa, (b) Δc, and (c) unit cell volume for neutron irradiation from different groups. Data includes results from Refs. 15 and 22. In parts (a) and (b) the error bars on the pure sample represent typical experimental error in determining lattice parameters. In part (c), the error bars represent the propagation of the error in the lattice parameters to the calculated V/V_0 value. All of our data in these plots should be considered to have comparable uncertainty.

$Mg_{1-x}Li_xB_2$ with the lithium substituting for the magnesium and no disruption of the boron sublattice.

The samples annealed at 500 °C for 1000 h suggest that at low levels, Li doping has little or no effect on H_{c2}. The 9.50×10^{18} cm^{-2} fluence sample has twice the amount of Li of the 4.75×10^{18} cm^{-2} fluence sample, yet their $H_{c2}(T=0)$ values are approximately equal and only slightly differ from the undamaged case. If the 18 T H_{c2} value seen for the 4.75×10^{18} cm^{-2} fluence level is truly a 2 T enhancement relative to the undamaged sample and is the result of Li doping, then we would expect the 9.50×10^{18} cm^{-2} fluence level to exhibit a $H_{c2}(T=0)$ near 20 T, which we did not observe. Since we cannot ensure that we have fully annealed out all of defects, it is possible that this slight increase in $H_{c2}(T=0)$ is a result of scattering associated with structural defects. In this case $H_{c2}(T=0)$ should be determined more by T_c than by the particular fluence level or post exposure annealing profile. The T_c values for the 4.75×10^{18} cm^{-2} fluence level annealed at 500 °C for 24 and 1000 h and that of the 9.50×10^{18} cm^{-2} fluence level annealed at 500 °C for 1000 h are all within half a degree of one another. This suggests that $H_{c2}(T=0)$ is controlled more by scattering associated with residual defects rather than any inadvertent Li doping. Since these low levels of Li do not appear to have any major impact on the superconducting properties, we can limit the discussion to possible influences of disorder, scattering, and possible changes in the Fermi surface.

The evolution of the superconducting transition temperature as a function of the unit cell dimensions (Δa, Δc, and V/V_0) shows definite trends and is in good agreement with the results of other neutron irradiation studies[15,22] (Fig. 18). Although there is considerable spread in the data, all three reports show that T_c tends to decrease with both Δa and Δc and hence V/V_0. These data show that, for neutron damaged samples, there is some correlation between the unit cell dimensions and the superconducting properties. They do not,

however, uniquely determine if the changes are a result of changes in the Fermi surface, perhaps due to a repositioning of the atoms, or if they are due to an introduction of additional scattering centers. In the case of substantial neutron-irradiation induced damage, where T_c is below 10 K, NMR measurements indicate that the suppression of superconductivity is the result of a decrease in the density of states of the boron $p_{x,y}$ orbitals.[46] This technique has been successful in experimentally determining a decrease in the density of states in $Mg_{1-x}Al_xB_2$ and AlB_2.[47,48] It should be noted, however, that measurements of the nuclear spin relaxation rate, T_1^{-1}, on ^{11}B yielded comparable T_1T values, which are directly related to the density of states at the Fermi surface, for both a neutron-irradiated sample that had a T_c near 7 K[46] and a sample with 30% aluminum substituted for magnesium that had a T_c near 25 K.[47] That the neutron damaged sample exhibits a dramatically lower T_c despite having virtually the same density of states at the Fermi surface suggests that additional mechanisms act to suppress superconductivity in neutron-irradiated MgB_2. This notion is supported by the fact that for the 24 h anneals at 300 °C, 400 °C, and 500 °C, the relative changes in the lattice parameters are fairly small. This should only contribute to minor changes in the Fermi surface, yet T_c is suppressed to near 25 K in the case of the 300 °C anneal.

Although there exist correlations between our data and literature reports on the evolution of T_c and the lattice parameters, the evolution of $H_{c2}(T=0)$ varies depending upon the irradiation conditions. This present work on heavily irradiated MgB_2 containing natural boron followed by post exposure annealing led to little or no enhancement of the upper critical field. In contrast, others have reported enhancements of H_{c2} for low fluence levels on MgB_2 containing either natural boron or isotopically enriched ^{11}B,[16,20] as well as fast neutron irradiation of natural boron containing MgB_2.[31]

In order to better understand this conspicuous difference, it is useful to review what happened during damage and subsequent annealing. When a neutron capture and subsequent alpha decay event occurs, the resultant damage is a large cluster of dislocations. Primary knock-on events cause a cascade of displacements that can be spread over a distance as large as 100 atomic distances.[14]

As mentioned previously, T_c suppression in as-damaged samples containing natural boron is much more rapid than those with either isotopically enriched ^{11}B or those that have been shielded from low energy neutrons. Therefore it is presumably the clusters associated with the neutron capture even that which are primarily responsible for the suppression of T_c. These clusters presumably have a low activation energy and can be largely repaired by the annealing process, which explains why we saw such a rapid increase in T_c for short time and low temperature anneals. In order to see an enhancement in H_{c2}, we need to anneal for a sufficient time and temperature so as to increase T_c to a level where we are not being limited by a low transition temperature. Since the defect clusters from the alpha decay of ^{11}B to ^{7}Li are presumably large, and we are relying on random diffusion to recombine vacancies and interstitials, higher reaction temperatures are necessary to restore T_c.

By going to higher annealing temperatures, we begin to repair defects with higher activation energies. Therefore, regardless of the actual energy associated with repairing the defects responsible for the enhancement of H_{c2}, we are most likely annealing many of them away while restoring T_c.

If it is these defects that are responsible for H_{c2} enhancement, then it is the annealing process that causes the different development of H_{c2} we observe.

Based on this analysis, it seems likely that a study of wire samples that have been exposed to much smaller fluences of neutrons (e.g., an exposure level that yields as damaged samples with a transition temperature in the range $30\ \mathrm{K} < T_c < 37\ \mathrm{K}$) should yield different, and higher, $H_{c2}(T)$ data.

The transmutation of ^{10}B following the absorption of a neutron results in the emission of an alpha particle of energy 1.7 MeV, which is quite comparable in energy to the 2 MeV He ion irradiation of MgB_2 films done by Gandikota *et al.*[28,49] One might therefore expect rather similar results between the two studies. A comparison of the results indicates that these two different types of irradiation give rise to different superconducting and normal state properties. Gandikota and co-workers irradiated with heavy ion fluences up to $1.2\times10^{17}\ \mathrm{cm}^{-2}$, which was sufficient to suppress T_c to below 5 K.[28] Unlike the case of heavy neutron irradiation presented here, He^{++} irradiation led to a slight enhancement in $H_{c2}(T=0)$ for samples exposed to lower fluence levels, where T_c was only suppressed by a few degrees,[49] analogous to the results obtained for lower fluence level neutron irradiation.[16,20] $H_{c2}(T=0)$ did tend to scale with T_c for samples with T_c below 30 K and, as with neutron-irradiated samples, $H_{c2}(T)$ begins to exhibit more WHH-like behavior when T_c in the vicinity of 10 K. Additionally, T_c could readily be restored by annealing at temperatures as low as 100 °C.[49] However, x-ray measurements indicated that the He ion irradiation did not change the *c*-lattice parameter, even for the highest fluence level.[28] Thus, He^{++} irradiation presumably creates more point defects rather than large defect clusters, which are likely to arise from neutron irradiation. He ion irradiation therefore presents yet another different avenue to systematically change the scattering levels in MgB_2.

Damage induced by neutron irradiation is fundamentally different from doping with aluminum or carbon. Both carbon and aluminum enter the structure and are believed to act as point defects in addition to electron doping the system. Arguments based on the temperature dependence of the anisotropy of the upper critical field suggest both carbon and aluminum doping increase scattering within the π band relative to the σ band, with the effect is much more pronounced in the case of carbon doping.[7] It should be noted that other researchers have concluded that changes in the temperature and magnetic field dependence of the thermal conductivity, $\kappa(T,H)$, for carbon substituted single crystals are consistent with carbon doping, resulting in an enhancement in intra-σ-band scattering.[50] Although there exists some debate as to the exact nature of the enhancement in scattering in carbon doped MgB_2, it is clear that the development of H_{c2} is dominated by scattering effects for carbon substitutions and Fermi surface changes effects for aluminum substitution. For neutron-irradiated samples, as discussed previously, the effects of the introduction of Li through nuclear processes are

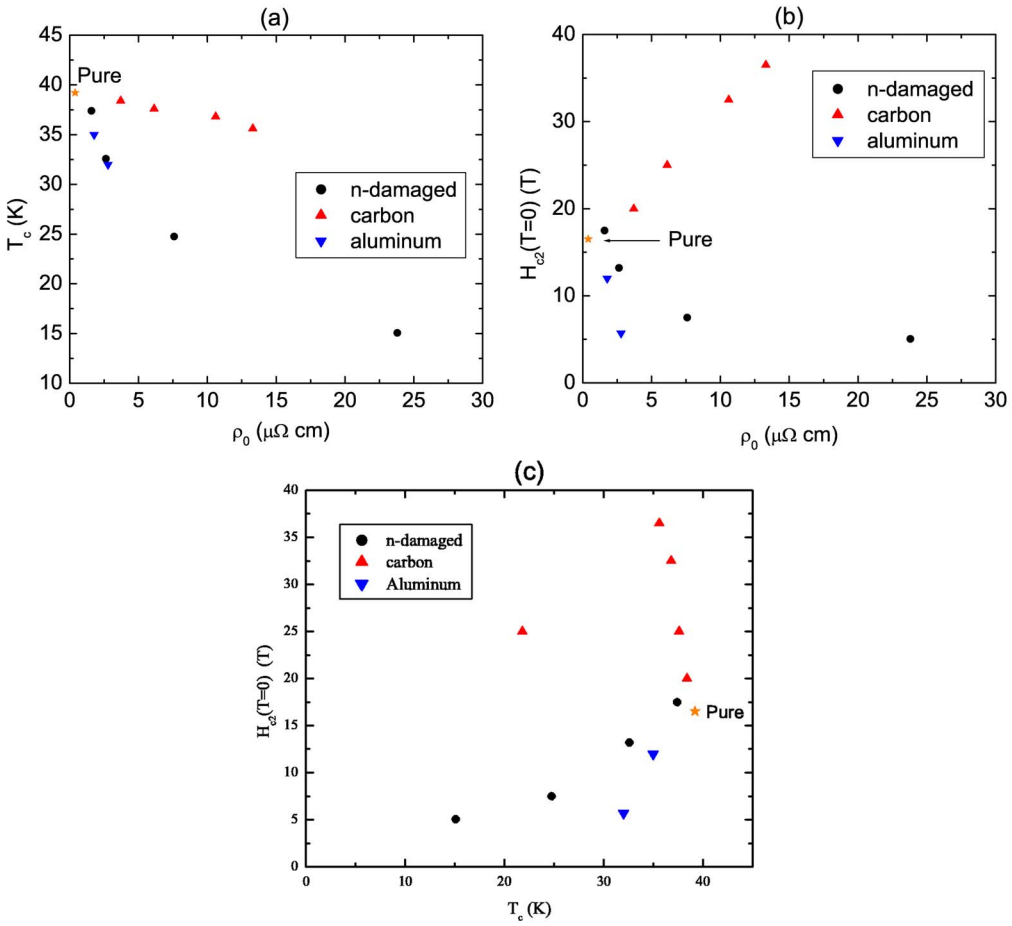

FIG. 19. (Color online) Interdependencies of T_c, H_{c2}(T=0), and ρ_0 for carbon doped (Refs. 25 and 51), aluminum doped single crystal (Ref. 9), and neutron-irradiated samples. (a) T_c vs ρ_0, (b) $H_{c2}(T=0)$ vs ρ_0, and (c) $H_{c2}(T=0)$ vs T_c.

negligible and the changes in the superconducting properties are due to an increase in interband scattering and a decrease in the density of states. Insights can be made into the effects of neutron-irradiated samples by comparison to carbon and aluminum doping.

The different development of interdependencies of $H_{c2}^{\|ab}$, T_c, and ρ_0 in aluminum doped,[9] carbon doped,[25,51] and neutron-irradiated samples, those exposed to a fluence of 4.75×10^{18} cm^{-2} and annealed for 24 h, are plotted in Fig. 19. Figure 19(a) shows the evolution of the transition temperature as a function of residual resistivity for these three types of perturbations. The suppression of T_c with ρ_0 for low resistivity values is quite similar for the neutron damaged and aluminum doped samples; T_c drops rapidly with increased scattering. In contrast, the suppression of T_c as a function of resistivity in carbon doped samples is quite gradual. This is consistent with both aluminum doping and neutron damaged samples, having more interband scattering than carbon doped compounds.

Figure 19(b) plots $H_{c2}(T=0)$ as a function of ρ_0. Here all three perturbations behave uniquely. The aluminum and neutron damage samples show a decrease in H_{c2}, whereas the carbon doped samples show a dramatic increases. The decrease in H_{c2} is more rapid in the aluminum doped samples than in neutron damaged samples. This can also be seen by plotting H_{c2} as a function of T_c (Fig. 19(c).

A direct comparison between the evolution of T_c and $H_{c2}(T=0)$ for carbon doping and neutron irradiation shows that the scattering associated with each type of perturbation is different. Within the model proposed by Gurevich,[11] enhancements in H_{c2} result from differences in the relative strength of scattering within each band, whereas the suppression of T_c is a function of scattering between the bands. The neutron-irradiated samples on these plots with a T_c greater than 25 K are samples that were annealed at 300 °C, 400 °C, and 500 °C. In each of these samples, annealing has reduced the a-lattice parameter to nearly the undamaged value (Fig. 2(b)). With the defect structure lying between nearly undamaged boron planes, one would not expect the scattering within the σ band to be substantially affected. If the scattering was confined primarily to the three-dimensional (3-D) π band, the resultant differences in intraband diffusivity values should manifest themselves in terms of enhanced H_{c2}. Since no significant enhancement is seen, we believe the scattering is primarily interband scattering and contributes to the suppression of T_c. The range in T_c for $V/V_0\sim1$ in post exposure annealed samples (Fig. 18(c)) supports the notion that neutron irradiation increases interband scattering.

The suppression in T_c in neutron-irradiated samples is the result of a combination of a decrease in the density of states at the Fermi surface and an increase in interband scattering.

In the case of aluminum doping, the suppression of T_c is believed to be primarily a result of a changes in the Fermi surface.[7] Samples of neutron damaged MgB_2 exhibit higher H_{c2} values than aluminum doped MgB_2 samples with similar T_c values (Fig. 19(c)). This suggests that, for neutron-irradiated samples, changes in the density of states suppress H_{c2} to a greater degree than interband scattering.

V. CONCLUSIONS

We systematically studied the effects of neutron fluence level, annealing temperature, and annealing time on the superconducting and normal state properties of MgB_2. As damaged samples showed an anisotropic expansion of the unit cell and a suppression of T_c to below 5 K. Defects introduced by the irradiation process had a relatively low activation energy and hence much of the damage could be repaired by post-exposure annealing. H_{c2} values tended to scale with T_c and the evolution of H_{c2} with ρ_0 was dramatically different than in the case of carbon doping. Lithium produced through nuclear processes appeared to have no significant effects on the superconducting properties. We attribute the changes in the superconducting properties of neutron-irradiated samples primarily to an increase in scattering between the two bands and possible changes in the density of state at the Fermi surface.

ACKNOWLEDGMENTS

Ames Laboratory is operated for the U.S. Department of Energy by Iowa State University under Contract No. W-7405-Eng-82. This work was supported by the Director for Energy Research, Office of Basic Energy Sciences. A portion of this work was performed at the National High Magnetic Field Laboratory, which is supported by NSF Cooperative Agreement No. DMR-0084173 and by the State of Florida.

[1] J. Nagamatsu, N. Nakagawa, T. Muranaka, Y. Zenitani, and J. Akimitsu, Nature (London) **410**, 6824 (2001).
[2] S. L. Bud'ko, G. Lapertot, C. Petrovic, C. E. Cunngingham, N. Anderson, and P. C. Canfield, Phys. Rev. Lett. **86**, 1877 (2001).
[3] J. Kortus, I. I. Mazin, K. D. Belashchenko, V. P. Antropov, and L. L. Boyer, Phys. Rev. Lett. **86**, 4656 (2001).
[4] R. A. Fisher, G. Li, J. C. Lashley, F. Bouquet, N. E. Phillips, D. G. Hinks, J. D. Jorgensen, and G. W. Crabtree, Physica C **385**, 49 (2003).
[5] Special invited review issue *Superconductivity in MgB_2: Electrons, Phonons and Vortices*, edited by G. Crabtree, W. Kwok, S. L. Bud'ko, and P. C. Canfield, Physica C **385** (1–2) (2003).
[6] R. J. Cava, H. W. Zandergen, and K. Inumaru, Physica C **385**, 8 (2003).
[7] M. Angst, S. L. Bud'ko, R. H. T. Wilke, and P. C. Canfield, Phys. Rev. B **71**, 144512 (2005).
[8] B. Kang, H. J. Kim, H. S. Lee, S. I. Lee, and T. Dahm, cond-mat/0409496.
[9] J. Karpinski, N. D. Zhigadlo, G. Schuck, S. M. Kazakov, B. Batlogg, K. Rogacki, R. Puzniak, J. Jun, E. Muller, P. Wagli, R. Gonnelli, D. Daghero, G. A. Ummarino, and V. A. Stepanov, Phys. Rev. B **71**, 174506 (2005).
[10] M. Putti, C. Ferdeghini, M. Monni, I. Pallecchi, C. Tarantini, P. Manfrinetti, A. Palenzona, D. Daghero, R. S. Gonnelli, and V. A. Stepanov, Phys. Rev. B **71**, 144505 (2005).
[11] R. H. T. Wilke, S. L. Bud'ko, P. C. Canfield, D. K. Finnemore, R. J. Suplinskas, and S. T. Hannahs, Phys. Rev. Lett. **92**, 217003 (2004).
[12] R. Puzniak, M. Angst, A. Szewczyk, J. Jun, S. M. Kazakov, and J. Karpinski, cond-mat/0404579.
[13] A. Gurevich, Phys. Rev. B **67**, 184515 (2003).
[14] A. C. Damask and G. J. Dienes, *Point Defects in Metals* (Gordon and Breach, Science Publishers, Inc., New York, 1963).
[15] A. E. Karkin, V. I. Voronin, T. V. Dyachkova, A. P. Tyutyunnik, V. G. Zubkov, Yu. G. Zainulin, and B. N. Goshchitskii, JETP Lett. **73**, 570 (2001).
[16] M. Eisterer, M. Zehetmayer, S. Tönies, H. W. Weber, M. Kambara, N. Hari Babu, D. A. Cardwell, and L. R. Greenwood, Supercond. Sci. Technol. **15**, L9-L12 (2002).
[17] E. Babic, D. Miljanic, K. Zadro, I. Kusevic, Z. Marohnic, D. Drobac, X. L. Wang, and S. X. Dou, Fiz. A **10**, 87 (2001).
[18] U. P. Trociewitz, P. V. P. S. S. Sastry, A. Wyda, K. Crockett, and J. Schwartz, IEEE Trans. Appl. Supercond. **13**, 3320 (2003).
[19] K. S. Krane, *Introduction to Nuclear Physics* (Wiley, New York, 1988).
[20] Y. Wang, F. Bouquet, I. Sheikin, P. Toulemonde, B. Revaz, M. Eisterer, H. W. Weber, J. Hinderer, and A. Junod, J. Phys.: Condens. Matter **15**, 883–893 (2003).
[21] M. Zehetmayer, M. Eisterer, J. Jun, S. M. Kazakov, J. Karpinski, B. Birajdar, O. Eibl, and H. W. Weber, Phys. Rev. B **69**, 054510 (2004).
[22] M. Putti, V. Braccini, C. Ferdeghini, F. Gatti, P. Manfrinetti, D. Marre, A. Palenzona, I. Pallecchi, C. Tarantini, I. Sheikin, H. U. Aebersold, and E. Lehmann, Appl. Phys. Lett. **86**, 112503 (2005).
[23] M. Ortolani, D. Di Castro, P. Postorino, I. Pallecchi, M. Monni, M. Putti, and P. Dore, Phys. Rev. B **71**, 172508 (2005).
[24] P. C. Canfield, D. K. Finnemore, S. L. Bud'ko, J. E. Ostenson, G. Lapertot, C. E. Cunningham, and C. Petrovic, Phys. Rev. Lett. **86**, 2423 (2001).
[25] R. H. T. Wilke, S. L. Bud'ko, P. C. Canfield, D. K. Finnemore, R. J. Suplinskas, and S. T. Hannahs, Physica C **424**, 1 (2005).
[26] R. A. Ribeiro, S. L. Bud'ko, C. Petrovic, and P. C. Canfield, Physica C **382**, 194 (2002).
[27] R. H. T. Wilke, S. L. Bud'ko, P. C. Canfield, D. K. Finnemore, R. J. Suplinskas, J. Farmer, and S. T. Hannahs, cond-mat/0507275.
[28] R. Gandikota, R. K. Singh, J. Kim, B. Wilkens, N. Newman, J. M. Rowell, A. V. Pogrebnyakov, X. X. Xi, J. M. Redwing, S. Y. Xu, and Q. Li, Appl. Phys. Lett. **86**, 012508 (2005).
[29] I. I. Mazin, O. K. Andersen, O. Jepsen, O. V. Dolgov, J. Kortus, A. A. Golubov, A. B. Kuz'menko, and D. van der Marel, Phys. Rev. Lett. **89**, 107002 (2002).

[30] J. M. Rowell, Supercond. Sci. Technol. **16**, R17 (2003).
[31] M. Eisterer, Phys. Status Solidi C **2**, 1606 (2005).
[32] N. R. Werthamer, E. Helfand, and P. C. Hohenberg, Phys. Rev. **147**, 295 (1966).
[33] M. Putti, M. Affronte, C. Ferdeghini, C. Tarantini, and E. Lehmann, cond-mat/050852.
[34] C. P. Bean, Phys. Rev. Lett. **8**, 250 (1962).
[35] M. Eisterer, M. Zehetmayer, and H. W. Weber, Phys. Rev. Lett. **90**, 247002 (2003).
[36] I. Pallecchi, C. Tarantini, H. U. Aebersold, V. Braccini, C. Fanciulli, C. Ferdeghini, F. Gatti, E. Lehmann, P. Manfrinetti, D. Marre, A. Palenzona, A. S. Siri, M. Vignolo, and M. Putti, Phys. Rev. B **71**, 212507 (2005).
[37] S. X. Dou, S. Soltanian, J. Horvat, X. L. Wang, S. H. Zhou, M. Ionescu, H. K. Liu, P. Munroe, and M. Tomsic, Appl. Phys. Lett. **81**, 3419 (2002).
[38] M. W. Thompson, *Defects and Radiation Damage in Metals* (Cambridge University Press, London, 1969).
[39] D. K. Finnemore, J. E. Ostenson, S. L. Bud'ko, G. Lapertot, and P. C. Canfield, Phys. Rev. Lett. **86**, 2420 (2001).
[40] A. A. Golubov and I. I. Mazin, Phys. Rev. B **55**, 15146 (1997).
[41] M. R. Eskildsen, M. Kugler, S. Tanaka, J. Jun, S. M. Kazakov, J. Karpinksi, and Ø. Fischer, Phys. Rev. Lett. **89**, 187003 (2002).
[42] A. F. Goncharov and V. V. Struzhkin, Physica C **385**, 117 (2003).
[43] X. H. Zeng, A. V. Pogrebnyakov, M. H. Zhu, J. E. Jones, X. X. Xi, S. Y. Xu, E. Wertz, Qi Li, J. M. Redwing, J. Lettieri, V. Vaithyanathan, D. G. Schlom, Zi-Kui Liu, O. Trithaveesak, and J. Schubert, Appl. Phys. Lett. **82**, 2097 (2003).
[44] S. Deemyad, T. Tomita, J. J. Hamlin, B. R. Beckett, J. S. Schilling, J. D. Jorgensen, S. Lee, and S. Tajima, Physica C **385**, 105 (2003).
[45] V. P. Antropov, K. D. Belashchenko, M. van Shilfgaarde, and S. N. Rashkeev, in *Studies of High Temperature Superconductors*, edited by A. Narlikar (Nova Science Publishers, Commack, NY, 2002), Vol. 38, p. 91.
[46] A. P. Gerashenko, K. N. Mikhalev, S. V. Verkhovskii, A. E. Karkin, and B. N. Goshchitskii, Phys. Rev. B **65**, 132506 (2002).
[47] S. Serventi, G. Allodi, C. Bucci, R. De Renzi, G. Guidi, E. Pavarini, P. Manfrinetti, and A. Palenzona, Supercond. Sci. Technol. **16**, 152 (2003).
[48] S. H. Baek, B. J. Suh, E. Pavarini, F. Borsa, R. G. Barnes, S. L. Bud'ko, and P. C. Canfield, Phys. Rev. B **66**, 104510 (2002).
[49] R. Gandikota, R. K. Singh, J. Kim, B. Wilkens, N. Newman, J. M. Rowell, A. V. Pogrebnyakov, X. X. Xi, J. M. Redwing, S. Y. Xu, Q. Li, and B. Moeckly, Appl. Phys. Lett. **87**, 072507 (2005).
[50] A. V. Sologubenko, N. D. Zhigadlo, S. M. Kazakov, J. Karpinski, and H. R. Ott, Phys. Rev. B **71**, 020501(R) (2005).
[51] Z. Holanová, J. Kačmarčík, P. Szabó, P. Samuely, I. Sheikin, R. A. Ribeiro, S. L. Bud'ko, and P. C. Canfield, Physica C **404**, 195 (2004).